

Development and evaluation of an external reusable piezo-based concrete hydration-monitoring sensor

Journal of Intelligent Material Systems and Structures

2019, Vol. 30(18-19) 2770–2788

© The Author(s) 2019

Article reuse guidelines:

sagepub.com/journals-permissions

DOI: 10.1177/1045389X19873414

journals.sagepub.com/home/jim



Sumedha Moharana¹  and Suresh Bhalla²

Abstract

Hydration of concrete is a very complicated and multiphase process, where the cement gel transforms into a hardened state from plastic/semiplastic phase. Proper progression of the hydration process ensures the development of targeted mechanical properties such as the elastic modulus, the coefficient of thermal expansion, the Poisson's ratio, and finally, the characteristic strength of concrete. Concrete experiences large thermal variations during the early phase of hydration due to the heat generated during the formation of cement hydration compounds, which contributes to shrinkage and cracking, somewhat making ground for the ultimate failure in the long run. Therefore, it is utmost important to monitor the progression of hydration for enhancing performance during the curing and the early service life. This article presents a new reusable external configuration of piezo-impedance transducers to monitor the hydration process in concrete structures using the electro-mechanical impedance technique. The proposed configuration consists of a thin metal foil instrumented with piezoelectric ceramic patch at the free end with the other end of the foil embedded inside the concrete. This configuration is compared against a piezoelectric ceramic patch directly bonded on the rebar used for reinforcement and another one embedded in the concrete surrounding the rebar. The sensing capability of the proposed metal foil configuration is clearly evident from the coupled admittance signature quantitatively vis-à-vis the other configurations. As a preliminary analysis, root mean square deviation values are employed to monitor the hydration process quantitatively. A piezo-equivalent mechanical model is also developed wherein the piezo-identified mass, stiffness and damping parameters are investigated for the cement hydration process so as to chalk out rigorous quantifiers of hydration progression. The employability of the proposed configuration is further proven by explanation of the physio-chemical products developed during various stage of hydration with step-by-step explanation along with correlation of the piezo-identified mass, stiffness and damping parameters. Overall, the proposed reusable configuration carries a high potential for field deployment in concrete industry for early detection of physio-chemical changes.

Keywords

Cement, concrete composite, hydration, lead zirconate titanate (piezoelectric ceramic), metal foil-based piezo sensor, electro-mechanical impedance technique

1. Introduction

Concrete is the most widely used building material in the construction industry. This is due to its low cost, easy availability and mouldability, which enhances its worth in most of the civil engineering applications. However, being a heterogeneous mixture of coarse aggregate, fine aggregate (sand) and cement, concrete has very complex nature of behaviour in terms of strength, durability and performance. Hydration of the cement paste is a very complicated physical and chemical process, which determines the microstructure of the hardened concrete (Bahador and Yaowen, 2010; Glisic and Simon, 1999; Neville, 2004; Tawie et al., 2010a). Concrete transforms from plastic to semi-plastic at the

hardened stage, sets and gradually gains major share of its strength during the hydration. During this process, compounds of cement (viz. the silicates of calcium, aluminium and iron, such as C_3S , C_2S , C_3A and C_4AF) react with water and forms various crystallized and anhydrous compounds such as ettringite, calcium

¹Department of Civil Engineering, Shiv Nadar University, Dadri, India

²Department of Civil Engineering, Indian Institute of Technology Delhi, New Delhi, India

Corresponding author:

Sumedha Moharana, Department of Civil Engineering, Shiv Nadar University, Dadri 201314, India.

Email: sumedha.maharana@snu.edu.in

silicate hydrate (CSH) gel and calcium hydroxide ($\text{Ca}(\text{OH})_2$) (Mehta and Monteiro, 2014; Neville, 2004). During the construction process (after casting, pouring and vibrating), strength monitoring is an important task to ensure the safety of both humans and structure. At the same time, strength monitoring also aids in determining the optimal time to demould the temporary framework, which carries substantial part in the overall budget of the construction project (Glisic and Inaudi, 2006). Various non-destructive evaluation (NDE) techniques such as ultrasonic pulse velocity, rebound hammer, acoustic emission and so on are conventionally employed in monitoring of the hydration process by measuring some property, indirectly related to the strength of concrete (Bahador and Yaowen, 2010; Soh and Bhalla, 2005). The conventional techniques for hydration monitoring are limited to certain extent for specific situations only. For example, the ultrasonic pulse velocity technique needs access of two sides of the structure for effective strength determination, which is in general infeasible for large structures, especially when the formwork is still present.

During the last and a half decades, the piezoelectric ceramic (PZT) patches have demonstrated their suitability for structural health monitoring (SHM) as sensors of the electro-mechanical impedance (EMI) technique for a wide variety of structures, including reinforced concrete (Bhalla et al., 2012; Bhalla and Soh, 2004a, 2004b, 2004c; Giurgiutiu and Zagari, 2000, 2002; Lim et al., 2006; Moharana and Bhalla, 2014; Park et al., 2000a, 2000b; Shanker et al., 2011; Soh et al., 2000; Sun et al., 1995; Talakokula et al., 2016). Basic concept of the EMI technique for SHM is to monitor the integrity of the structure by measuring the electrical admittance via the PZT transducer bonded on the surface of the monitored structure. Because of the direct and the converse piezoelectric effects, any change in the mechanical impedance of the structure caused by damage modifies the electrical admittance of the PZT transducer bonded to it. Usually, the electro-mechanical admittance signature, comprising of the conductance (real part) and the susceptance (imaginary part) is acquired in the healthy condition of the structure and used as the reference baseline for future decisions on structural integrity. Any occurrence of damage on the structure modifies the admittance signature, thereby providing a signal to the end user. Bhalla and Soh (2004b, 2004c) developed a two dimensional piezo-impedance approach based on the concept of effective impedance to model the PZT–structure interaction manifesting active and passive part of coupled admittance signature. Any damage to the structure will cause these characteristics to change and hence changes the structural impedance ($Z_{s, \text{eff}}$), which in turn alters the Electrical admittance (\bar{Y}) as given by the following expression

$$\bar{Y} = \frac{\bar{I}}{\bar{V}} = G + Bj = 4\omega j \frac{l^2}{h} \left[\frac{\bar{\epsilon}_{33}^T}{\epsilon_{33}^T} - \frac{2d_{31}^2 \bar{Y}^E}{(1-\nu)} + \frac{2d_{31}^2 \bar{Y}^E}{(1-\nu)} \left(\frac{Z_{a, \text{eff}}}{Z_{s, \text{eff}} + Z_{a, \text{eff}}} \right) \left(\frac{\tan kl}{kl} \right) \right] \quad (1)$$

where ω is the angular frequency, l the half-length and h the thickness of the patch; $\bar{\epsilon}_{33}^T = \epsilon_{33}(1 - \delta j)$ the complex piezoelectric permittivity (δ being the dielectric loss factor); $\bar{Y}^E = Y^E(1 + \eta j)$ the complex Young's modulus (η being the mechanical loss factor); $Z_{s, \text{eff}}$ and $Z_{a, \text{eff}}$ respectively, the effective impedances of the structure and the PZT patch; and k the wave number. This equation couples the mechanical impedance of the structure with the electrical admittance \bar{Y} , which means that any damage to the structure (change of $Z_{s, \text{eff}}$) will reflect itself as change in \bar{Y} . Furthermore, a continuum approach has recently been developed with rigorous inclusion of the bonding effect on the coupled admittance signature (Moharana and Bhalla, 2014, 2015).

As an extension of SHM, several researchers have studied the possible deployment of smart materials, especially optical fibre sensors and PZT patches, for monitoring of cement concrete hydration in surface bonded and embedded configurations. During late 1990s, Glisic and Simon (1999) developed an experimental method to monitor concrete deformations at early stage of construction using Surveillance d'Ouvrages par Fibres Optiques (SOFO) sensors. Subsequently, they also reported the limited application of SOFO sensor for in situ concrete hydration measurement. Azenha et al. (2009) monitored the thermal deformation and shrinkage during early stage cement hydration using electrical strain gauges. A thermo-mechanical numerical model was developed to simulate the early-age concrete behaviour of the specimen.

Soh and Bhalla (2005) proposed PZT identified stiffness as an indicator of hydration progress. The equivalent stiffness parameter (ESP) was found to be more sensitive to hydration as compared to the ultrasonic pulse velocity measurement. Shin et al. (2008) investigated the applicability of the EMI technique for strength gain monitoring of early-age concrete. PZT patches were employed as EMI sensors to monitor the curing of concrete. They reported good experimental results showing excellent potential of the EMI sensing technique as a practical and reliable NDE technique for concrete strength gain monitoring. Shin and Oh (2009) investigated the potential use of the PZT patches for concrete strength monitoring in surface bonded mode. However, the moisture loss in concrete plays a greater role in volumetric shrinkage, which could mislead the overall admittance signature of sensor in the surface bonded configuration. Hence, their approach was not full proof complete. Tawie et al. (2010b) studied the hydration progression in cement paste using

reusable piezo sensor bonded on a plate. They successfully monitored the physical changes occurring during hydration and quantified the same through the root mean square deviation (RMSD). However, the analysis was restricted to the real component of the admittance (i.e. conductance) signature only. Tawie and Lee (2010) employed the PZT patches bonded to steel reinforcement and embedded in concrete. They reported the significant changes in curing characteristics of concrete for varying water–cement (w/c) ratio, compaction methods and curing regimes. They reported that the shifting of the piezo-coupled resonance peak and the frequency change is more significant between the setting and the hardening phase. Bahador and Yaowen (2010) developed a unique approach to arrest the actual densification and volumetric shrinkage during concrete hydration through an encompassed reusable PZT patch. This consisted of a piece of PZT patch bonded to an enclosure with two bolts tightened inside the holes drilled in the enclosure. They also included an embedded sensor in their study. They concluded that the embedded piezo sensor is quite sensitive to capture the initial hydration process whereas enclosed configuration of the reusable PZT patch can be used for monitoring the setting of the fresh concrete. Wang and Zhu (2011) proposed an experimental technique to monitor and predict the early-age strength of concrete through statistical interference of the mean average percentage deviation and the RMSD indices using waterproofed PZT sensors embedded in concrete. Ni et al. (2012) developed a NDE technique based on the propagation of highly nonlinear solitary waves to monitor the hydration of cement. Their studies mostly focused on monitoring granular crystal formation of the hydrated product during the strength gain period. However, main limitation arises here due to piezo induced surface waves in heterogeneous concrete. From the experimental outcomes, they concluded that the proposed technique is more reliable for hydration monitoring during early age only. Providakis and Liarakos (2014) developed a portable and innovative telemetric EMI monitoring system to monitor concrete strength development ranging from the initial stages of casting to the final 28 days cured stage. They found that the EMI technique is very sensitive to the strength gain of concrete structures right from the earliest stages.

In recent years, many researchers investigated concrete strength monitoring process for concrete foundations through precast blocks using embedded smart aggregates using the wave propagation approach (Constantin et al., 2016; Lim et al., 2018a, 2018b; Lu et al., 2017, 2018). From the experimental results, they found that harmonic amplitude variation measured by the piezo sensor is the key index related to concrete strength development (Banerjee et al., 2009; Sikdar and Banerjee, 2016). Furthermore, they developed wireless sensory network for remote strength gain monitoring.

Kong et al. (2013) successfully identified three different phases (the fluid state, the transition state and the hardened state) during the hydration process of concrete through piezo wave propagation approach. Different amplitude and constant frequency sine wave excitations were used for characterization and monitoring process of concrete. Su et al. (2016) demonstrated a real time in-site monitoring of hydraulic concrete strength using PZT smart module pairs through wave propagation approach. A mathematical model was developed through mapping between the stress wave amplitude data and the fuzzy inference approach to formulate a relationship between concrete strength and the stress wave amplitude.

All the above described studies involved PZT patches either surface bonded or embedded configuration. Although reusable type of sensors have been proposed, their fabrication and instrumentation tended involved partial/full embedment in concrete. This article proposes a new PZT-based reusable hydration-monitoring sensor with the sensor remaining external to the concrete structure to be monitored. The sensor uses a very simplified configuration consisting of a hanging metal foil as compared to all past demonstrations, which allows dismantling the sensor externally without any damage to concrete. It consists of a PZT patch bonded at the end of metal foil, whose other end is embedded inside concrete during casting. The article evaluates the proposed configuration vis-à-vis the previously tested configurations, namely, the surface bonded, the embedded and the one bonded to the inserted steel bar. The coupled piezo-impedance signatures are acquired from the lab-sized concrete samples for 70 days in regular fashion for monitoring the strength gain and hydration phases of concrete. The equivalent structural parameters have been determined using effective impedance approach to establish the relation between the cement concrete setting and hardening stages and sensor identified structural properties during continuous hydration. Monitoring the concrete strength or hydration at early stage construction is otherwise very difficult due to lack of accessibility. The forthcoming sections of article cover experimental details, analysis and result interpretation related to the hydration.

2. Experimental details

As part of the experimental investigation, three concrete cube samples ($150 \times 150 \times 150 \text{ mm}^3$ in size) were prepared using M30 concrete mix in accordance with IS 10262 (2009), as shown in Figure 1. The ingredients (Cement: Water: Coarse Aggregate: Fine Aggregate) were proportioned as 1:0.44:2.74:1.34 in accordance with the mix design procedure. The aggregate sampling and their size grading has been

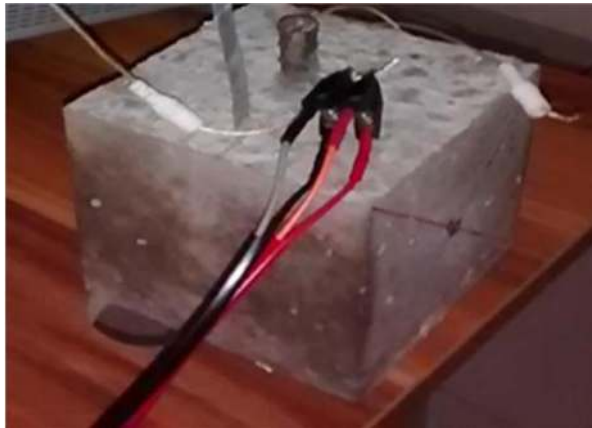


Figure 1. A typical concrete specimen instrumented with PZT patches in different sensor configurations.

confirmed to IS 383 (1970). The nominal size aggregate used for this mix is 20 mm. The PZT patches were instrumented on the concrete cubes in three different configurations for the purpose of evaluation: (a) embedded in the concrete surrounding the rebar (Figure 2(a)), (b) bonded to steel rebar embedded inside

concrete as reinforcement (Figure 2(b)) and (c) attached at the end of an aluminium foil in turn embedded inside concrete (Figure 2(c)). Soft PZT transducers of grade of PIC 151 (manufactured by PI ceramic) of size of $10 \times 10 \times 0.3 \text{ mm}^3$ were used for all the three sensor configurations. All the piezo configurations were ready prior to casting and installed during the casting. All the PZT transducers were bonded using a thin layer of Araldite epoxy adhesive. In order to protect the patches (rebar and metal foil configurations) from water during casting, an additional layer of the Araldite epoxy was applied on top of the sensors as a durable cover (see Figure 2(b) and (c)). Figure 3 presents the complete laboratory setup for the overall experimental programme.

For this study, the authors have evaluated a new piezo configuration, metal wire-based EMI (MWBEMI) variant for hydration monitoring of concrete for the first time. In the proposed setup, the PZT patch is not directly bonded on the surface of the structure but operates from the end of the steel wire in turn attached to the concrete sample, as shown in Figure 2(c). A thin aluminium foil of length 508 mm and cross-section of $10 \times 1 \text{ mm}^2$ has been used. One end

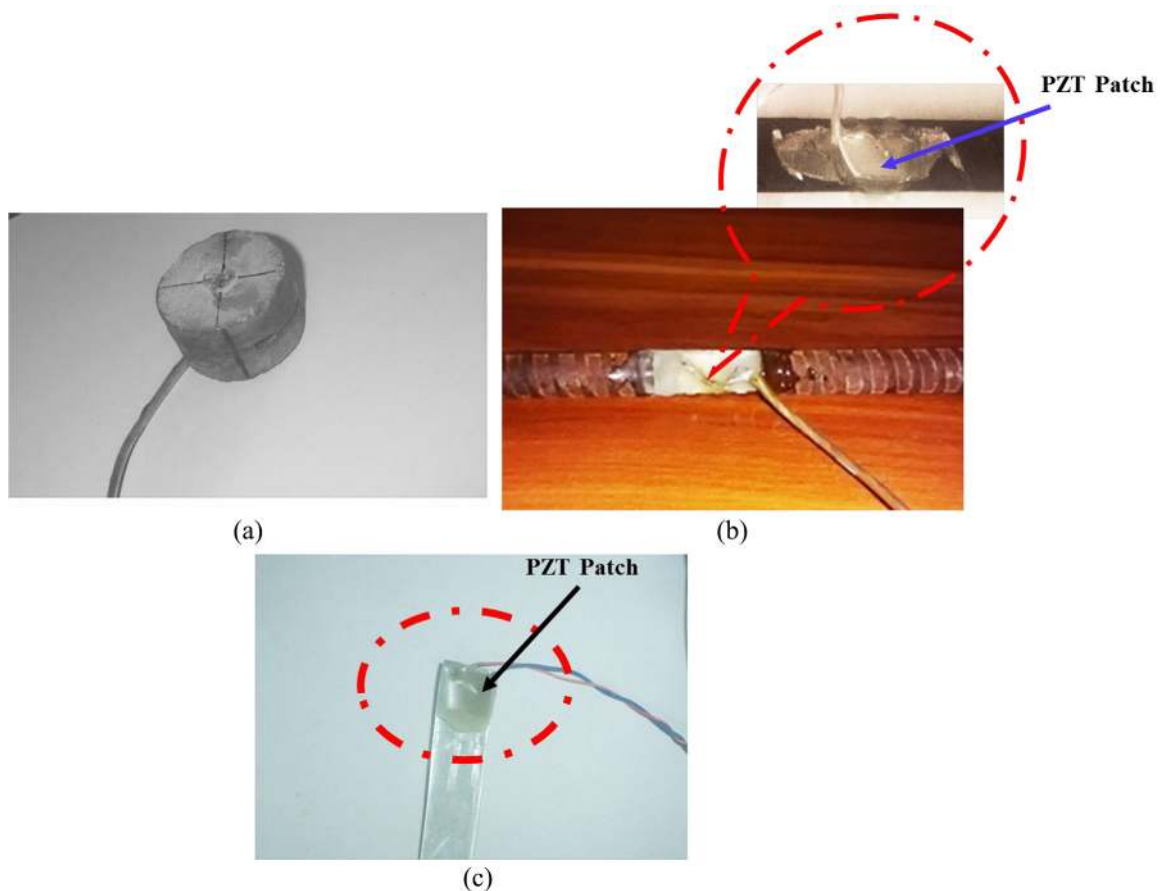


Figure 2. Various sensor configurations considered in study: (a) Embedded PZT patch in the form of CVS, (b) PZT patch bonded to steel bar and (c) PZT patch bonded to metal foil.

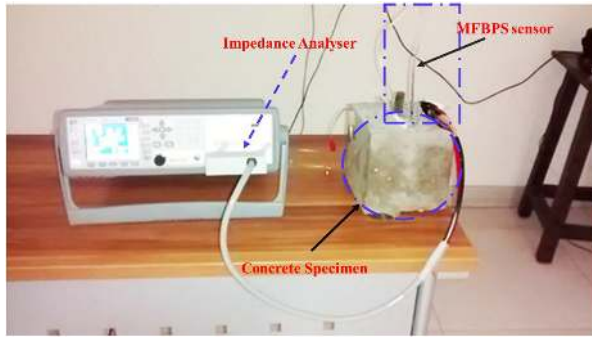


Figure 3. Experimental setup in laboratory.

of aluminium foil was inserted into the concrete sample (up to 50 mm from the top surface) and other end a PZT patch bonded the foil, as shown in Figure 2(c). PZT patches were $10 \times 10 \times 0.3 \text{ mm}^3$ in size and conformed to grade PIC 151 (PI Ceramics, 2017). In this configuration, although the sensitivity of the piezo-coupled structural interaction gets compromised, the MWBEMI variant is a panacea in situations (such as complex junction of rail bridge girder, pier caps) where implementation of the traditional EMI technique is not feasible. Another advantage of using the MWBEMI technique is that since the PZT patches are attached at the end of the metal wire, resonance at certain frequencies are virtually maintained regardless of the nature of the host structure, which is otherwise a matter of concern in materials with high damping, such as concrete and certain ceramics. Hence, resulting signature consisting of peaks is somehow guaranteed, which renders damage detection relatively easier visually. The effectiveness of this configuration of piezo sensor is higher degree of reusability. As the PZT patch has been attached to end of the metal foil, the foil can be easily cut from the embedded part and can be reutilized any other structure for monitoring purpose. This flexibility is not available on previously demonstrated reusable sensors which entailed partial/ full embedment implying that reusability would need damage to concrete.

As can be observed from equation (1), when structural properties goes through rheological changes (hence $Z_{s, \text{eff}}$), the coupled EMI of the PZT patch undergoes variations. Any change in the conductance signature, such as magnitude or frequency shift, is attributed to the underlying structural changes and hence the impedance. In the present context, the shifts would reflect the structural changes occurring in concrete due to hydration.

Among the above configurations, the surface bonded configuration is the most widely researched so far. It is, however, plagued by issues such as vulnerability to environment degradation, besides the absence of a perfectly flat surface of concrete, which tends to undermine bonding. Hence, for this study, the surface bonded

configuration has avoided. Bonding the PZT patch to the rebar (Figure 2(a)) provides an alternative configuration which ensures protection to the patch. It has been successfully demonstrated to be effective in the progression of chloride and carbonation induced corrosion (Talakokula et al., 2014, 2016). The embedded configuration (see Figure 2(c)) was achieved by means of concrete vibration sensor (CVS), a ready-to-use piezo-cement composite developed at the Smart Structures and Dynamics Laboratory (Bhalla and Gupta, 2007) and recently demonstrated to be suitable for rebar corrosion monitoring (Talakokula and Bhalla, 2015), especially during the early stages. Its advantages, aside from protection to the otherwise fragile PZT element, include easy installation as well as better strain integration with surrounding concrete of the structure. Recently Kaur and Bhalla (2015) also demonstrated the CVS for combined SHM and energy harvesting from an RC structure. Tawie and Lee (2011) proposed a novel reusable PZT sensor, comprising a PZT patch attached on a bolt. The sensor is installed on the rod embedded in the cement mortar and can be taken off for reuse after measuring the EMI. The metal foil-based configuration (Figure 2(c)) stems as an adaptation of the metal wire-based configuration originally proposed by Na and Lee (2013) and recently improved upon by Naskar and Bhalla (2015) by replacing the wire by a metal foil. It offers advantages such as reusability, generation of peaks even in highly damped material like concrete and being semi-remote in application. Lu et al. (2017) developed a novel impedance-based model based on concept of Smart Probe (PZT patch bonded on first surface bonded on a pre-fabricated aluminium beam). They found the dynamic modulus of elasticity of the host structure from the conductance signatures using the proposed model and demonstrated the superiority of the proposed technique with excellent repeatability test.

The present investigation that involves the metal foil-based configuration, intended to be a reusable hydration sensor is the first ever application of the metal wire configuration in concrete, especially for hydration monitoring with aid of piezo equivalent parameters. It consists the instrumented concrete specimen, an LCR metre (Agilent 4980A, 30–300 kHz range) and a laptop equipped with data acquisition software (VEEPRO 9.2). The EMI signatures of the PZT patches for all the three specimens were acquired by measuring conductance and susceptance of the patches for the frequency range of 50–300 kHz at an interval of 100 Hz. Sun et al. (1995) recommended a frequency band (40–300 kHz) containing major vibrational modes of the structure for EMI-based monitoring, that is, large number of peaks in the signature. Park et al. (2003) recommended a frequency range from 30 to 400 kHz for PZT patches 5–15 mm in size employed for piezo-based SHM. According to Park

and coworkers, a higher frequency range (>200 kHz) is favourable in localizing the sensing range, while a lower frequency range (<70 kHz) covers a large sensing area.

The EMI signatures were recorded every hour for the initial 12 h and has been monitored for next 28 days. The curing of sample was done in the indoor atmospheric conditions within the temperature range of 28°C ± 2°C and consistent humidity. The following section covers detailed observations based on visual analysis of signature and the use of statistical quantification based on variations in the raw conductance signature.

3. Statistical analysis of conductance signatures

Several statistical parameters can be used to quantify the changes in signature resulting from structural change (concrete rheological change) utilizing the raw conductance signatures. In this study, the RMSD index was used to statistically quantify the changes in the signature occurring during the hydration. At preliminary level, the main effects of any structural damage or change in material characteristic on the signature are the horizontal and the vertical shifts and also the resulting frequency shifts with respect to the free PZT plots (Jung et al., 2014; Lim et al., 2006; Mascarenas et al., 2010). These are the main indicators for physiochemical change in concrete. The RMSD of the conductance signatures can be computed here for damage quantification, as given by

$$RMSD(\%) = \frac{\sqrt{\sum (G_i - G_0)^2}}{\sum G_0^2} \times 100 \quad (2)$$

where G_0 is the baseline conductance value and G_i the corresponding current conductance at the i th measurement point.

For the sake of standardization of hydration results (i.e. 28 day of curing), the RMSD results were plot for 28 days only. In general, for all the three configurations, initially sharp peaks were observed at the PZT patch's resonant frequencies, which flattened (coupled with up/down and lateral shifting) with the passage of time, when concrete transitioned from the plastic to the hardened state (Lee and Tawie, 2009; Lim, 2014; Tawie et al., 2013). Large shifts in signatures were observed during the first 40 h. After that, the shifts were very gradual, indicating that concrete attains most of its stiffness during the initial hours followed by nominal changes. The specific observations are described with the aid of Figures 4 to 8 as follows. The coupled admittance signatures for all three configuration are plotted for long-term hydration and early hydration phases, respectively.

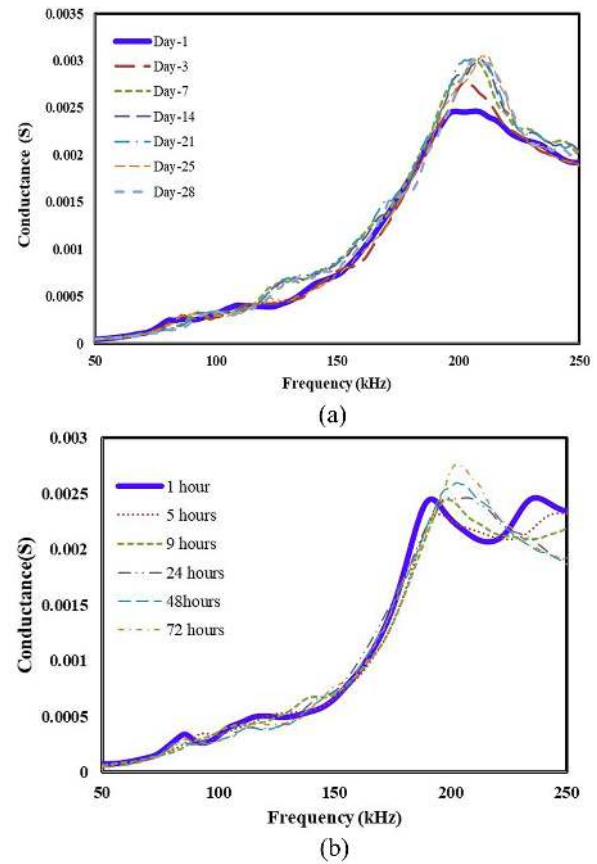


Figure 4. Compilation of conductance signature obtained from embedded configuration for concrete Specimen I during hydration: (a) long-term hydration and (b) early hydration.

Figure 4 shows the conductance plot of the embedded CVS for Specimen 1. For this sensor, the strength gain and densification can be significantly interpreted from overall deviation in conductance signature as well as the piezo patch's resonance peaks, which can be observed through shifting peaks rightwards and also attain higher conductance values as the hydration process progressed. Similar behaviour has been observed for both long-term (see Figure 4(a)) and early hydration monitoring of cement concrete by many researchers (see Figure 4(b)) (Kim et al., 2015; Lim et al., 2016; Talakokula and Bhalla, 2015; Tawie et al., 2010a, 2010b; Tawie and Lee, 2010; Thiagarajan et al., 2017; Yang et al., 2008, 2012).

Figure 5 shows the corresponding signatures for the PZT patch bonded on the rebar. For this patch, the resonance peaks for first few hours (plastic and transition periods) can be observed to descend (during early hydration, see Figure 5(b)), shifts right and then significantly move upwards (Cheol and Park, 2016; Jung et al., 2014; Lim, 2014; Park et al., 2008; Talakokula et al., 2018). Figure 6 shows the corresponding plots of the metal foil-based piezo sensor (MFBPS) configuration. For this case, the resonance peaks of the

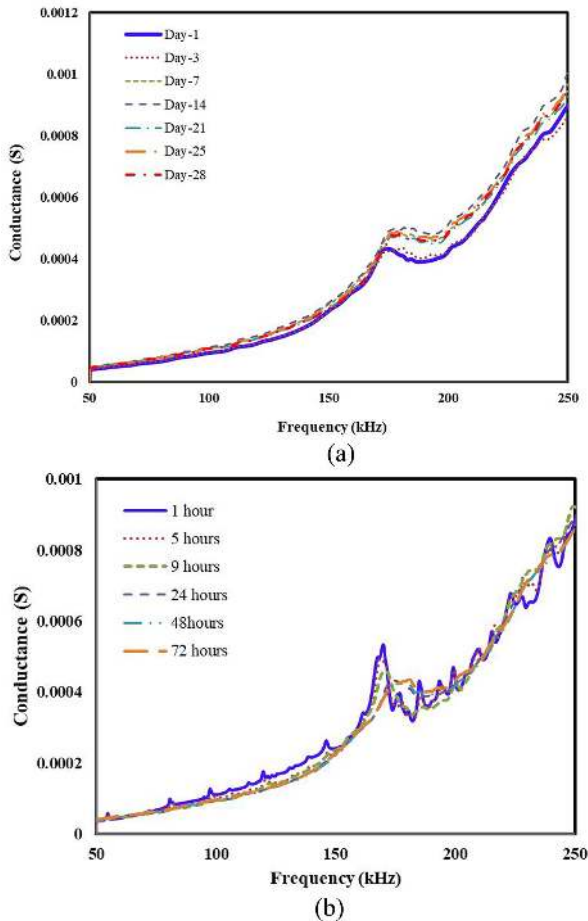


Figure 5. Compilation of conductance signatures obtained for rebar bonded configuration for Specimen I during hydration: (a) long-term hydration and (b) early hydration.

conductance signatures significantly increase in magnitude throughout the process hydration entailing solidification, densification and hardening. Figure 6(b) represents the early hydration signatures of concrete sample and signatures are coherent with long-term hydration results (continuously increasing in conductance value). The continuous increase in the resonance peak demonstrates its excellent capability to monitor the strength gaining process of concrete. Hence, it can be widely used for monitoring and damage identification techniques for those structures where accessibility is the main challenge.

In general, the observations are consistent to that reported by Soh and Bhalla (2005), who theorized that the relative shift of piezo peak as compared to ‘free-free’ condition essentially reflected the gradual gain in the strength of concrete caused by hydration of concrete (Lee and Tawie, 2009; Tawie et al., 2013). Similar behaviour of these sensor types was observed for Specimens 2 and 3, as can be observed from Figures 7 and 8 for both early hydration and long-term hydration monitoring. Figure 9 represents the typical USPVP results of

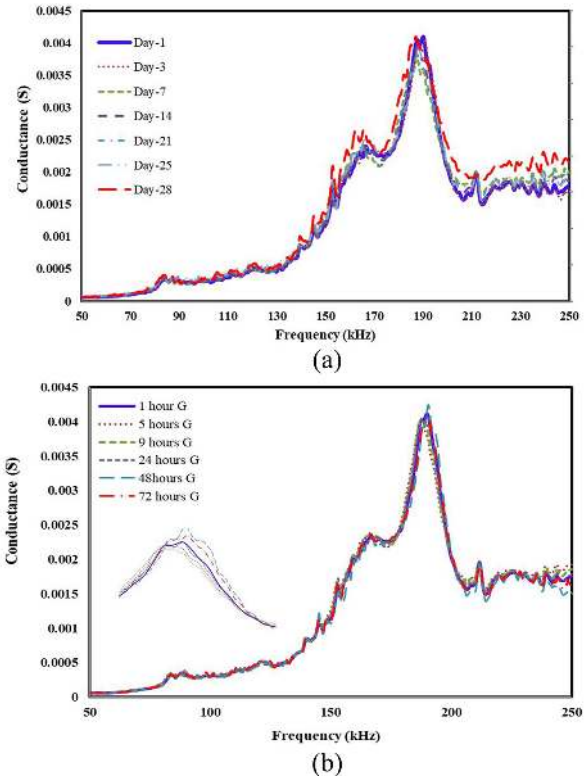


Figure 6. Compilation of conductance signatures obtained from MFBPS configuration for Specimen I during hydration: (a) long-term hydration and (b) early hydration.

concrete samples monitored for hydration. The results trend shows concrete solidification in overall hydration process.

Since the real part actively interacts with the structure, it is traditionally preferred over the imaginary part for preliminary analysis involving RMSD index. The RMSD variation (see equation (2)) is plotted over the 28-days hydration period for all the sensor configuration in Figures 10 to 12 for Specimens 1, 2 and 3, respectively. From these figures, it is observed that initially, the RMSD values increase significantly due to the rapid setting of concrete but thereafter attain more or less constant values with time. Except for the magnitude, the trend of RMSD is similar for all piezo-configurations. However, significant number of outlier points can also be observed. This is a well-accepted drawback of a statistical indicator like RMSD (Park et al., 2003; Soh and Bhalla, 2005; Talakokula et al., 2016). It also does not provide a quantitative indicator for the degree of hydration achieved. The variation of the RMSD values for the MFBPS configuration is essentially similar to other piezo configurations, though its magnitude is somewhat lower. The raw conductance signature RMSD variation for the embedded and the steel rebar configuration or concrete hydration are already established by many researchers (Park et al., 2003; Soh and

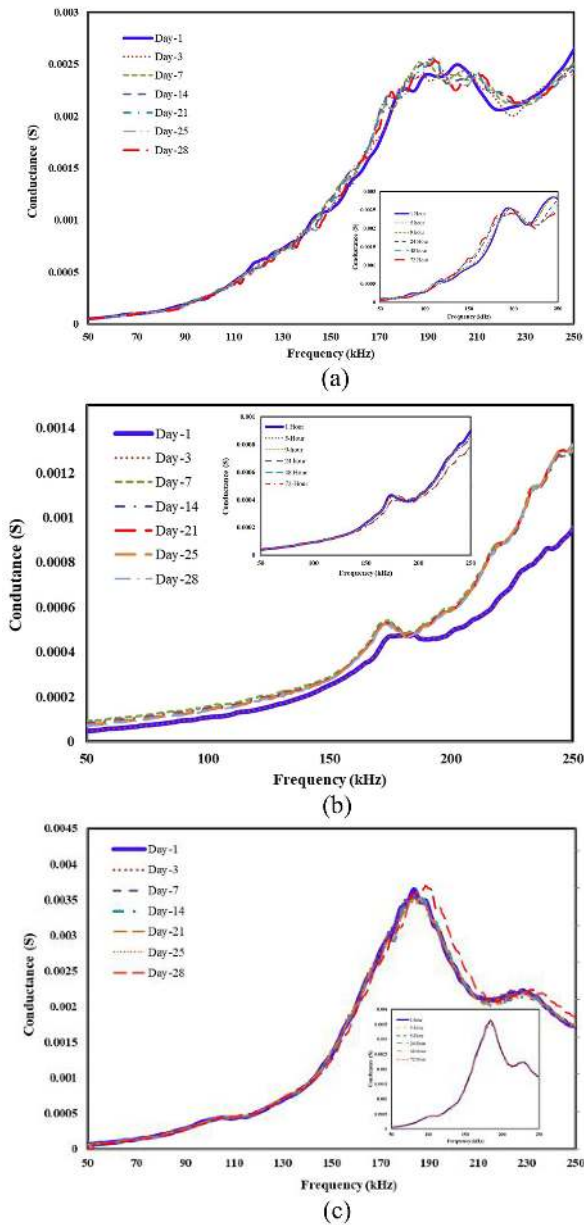


Figure 7. Compilation of conductance signature for concrete Specimen 2 for (a) embedded configuration, (b) rebar bonded configuration (c) MFBPS configuration.

Bhalla, 2005; Talakokula et al., 2016), the current study, focused on MFBPS configuration only. The raw-signatures and the RMSD curves acquired for MFBPS configuration display satisfactory performance as like other piezo configurations. However, RMSD is suitable for preliminary level of interpreting the changes in signatures. It does not provide a strong means of quantifying changes on a uniform scale or in parametric form. After visual and statistical correlations and establishment of the MFBPS external configuration for hydration, the next step is to derive definite quantitative indicators of hydration suitable for field application. This is covered in the next section.

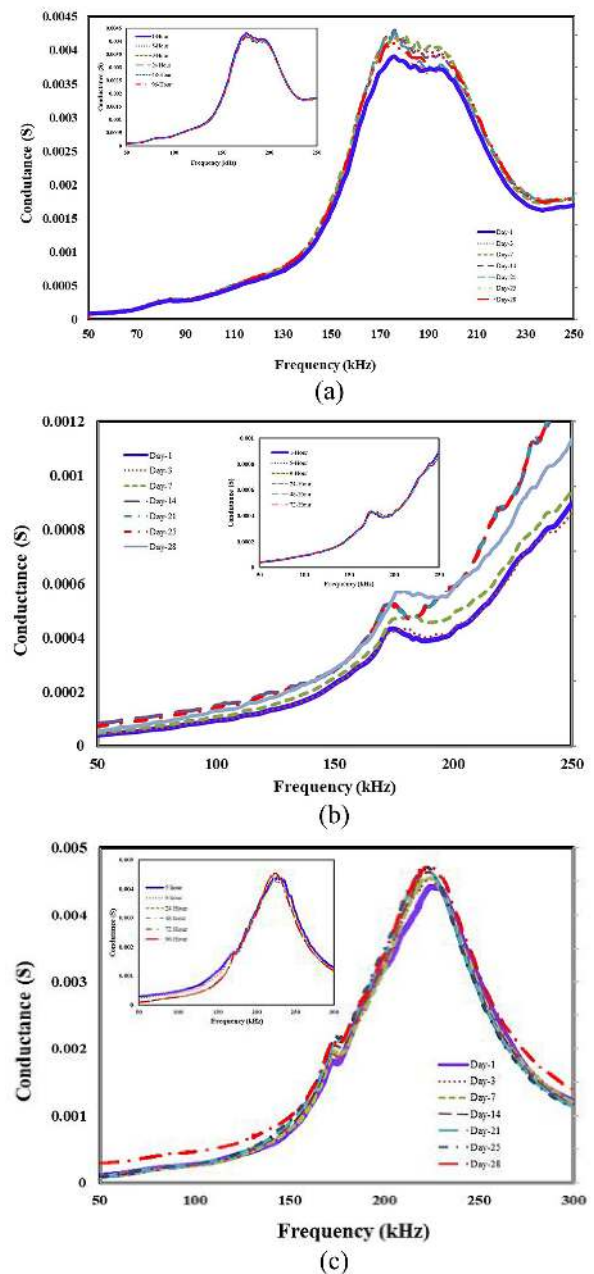


Figure 8. Compilation of conductance signature for concrete Specimen 3 for (a) embedded configuration, (b) rebar bonded configuration and (c) MFBPS configuration.

4. Analysis based on impedance-based structural identification

In order to gain a deeper insight into structural changes occurring in concrete related to stiffness, mass and damping induced by concrete hydration, impedance approach was employed for structural identification for the metal foil-based PZT patch. This study only considers the MFBPS configuration for overall piezo-identified system model as sufficient literature is already available related to other two configurations

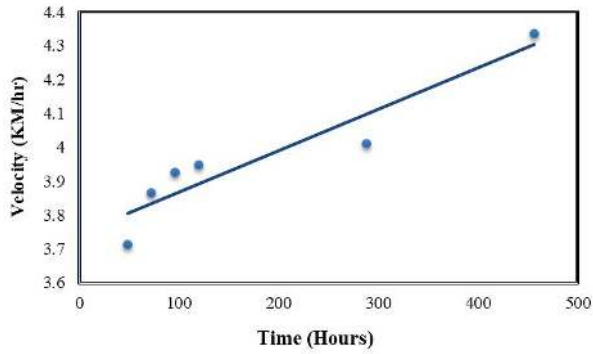


Figure 9. USPV test results of concrete specimen.

(Bhalla et al., 2012, 2017; Soh and Bhalla, 2005; Talakokula et al., 2016). The experimental signatures of the MFBPS-based PZT patches for the three specimens consist of the real and the imaginary components, G and B , respectively, over 50–300 kHz range. The mechanical impedance of the host structure was obtained at each frequency using equation (1) through the already established computational procedure (Talakokula et al., 2016). The extracted mechanical impedance ($Z_{s, eff} = x + jy$) consists of the real and the imaginary components, x and y , respectively, the variation of which with frequency provides a clue for system identification and carries vital information related to the parameters of the structure encompassing mass, damping and stiffness (Hixon, 1988). For this purpose, it is a prerequisite to study the impedance patterns of few simple systems and select which fits best for the particular case as per the guidelines of Bhalla et al. (2017). For MFBPS configuration, a close examination of the extracted impedance components in the frequency range 170–180 kHz in the initial hours of hydration revealed that the system behaviour is similar to that of the combination of basic elements shown in Table 1 (Bhalla and Soh, 2004b, 2004c). For system parameter identification from extracted impedance spectra, the frequency range 170–180 kHz has been chosen since the system behaviour was found to be similar to a parallel spring-damper (k - c) combination, in series with mass ' m '. From Figures 13 to 15, it can be seen that the comparison between the experimental plots with the analytical plots for this equivalent system holds a satisfactory agreement. Hence, the structural system is identified with a reasonably good accuracy.

This system consists of a series combination of a mass element (m) with a damper (c), the combination then being in parallel with a spring (k). The next step that follows is the quantitative determination of the parameters m , c and k , henceforth referred to as the 'equivalent' parameters of the host structure, here the concrete block. It may be noted that these parameters are obtained through experimental data directly,

without any prerequisite for material or geometrical details of the specimen or any 'model' of the system. After algebraic rearrangement of the expressions given in Table 1, following expressions can be derived with equivalent structural parameters (Bhalla et al., 2017)

$$c = \frac{x_0x_1\omega_1^2 - x_0x_1\omega_0^2}{x_0\omega_1^2 - x_1\omega_0^2} \quad (3)$$

$$m = \left[\frac{x_0(x_0x_1\omega_1^2 - x_0x_1\omega_0^2)^2}{(x_0\omega_1^2 - x_1\omega_0^2)(x_0x_1\omega_0^2\omega_1^2 - x_0\omega_0^2\omega_0^2)} \right]^{\frac{1}{2}} \quad (4)$$

$$k = \frac{m^{-2} - y\omega(c^{-2} + (\omega m)^{-2})}{c^{-2} + (\omega m)^{-2}} \quad (5)$$

where $x = x_0$ is the peak magnitude of conductance at $\omega = \omega_0$. $x = x_1$ (somewhat less than the peak magnitude) is the value of the component x at $\omega = \omega_1$ ($< \omega_0$). The values of ω_0 and ω_1 are 171 and 179 kHz, respectively, for Samples 1 and 2. Hence, adopted similar trend for Sample 3.

The extracted structural impedance components (x vs f and y vs f) have been plotted over the chosen frequency range resulting from the equivalent parameters and compared with the experimental values of x and y in Figures 13 to 15. All the piezo-identified structural parameters have been plotted for 28 days after casting for better evaluation. They are remarkably matching each other as can be observed from the three figures. These extracted piezo-identified parameter for other sensor location (embedded and bonded with steel bar) for concrete strength gain and other properties has already been studied rigorously (Talakokula and Bhalla, 2015; Talakokula et al., 2016). Hence, the focus of this study to evaluate the PZT identified mass, spring and damping values only for the PZT patch bonded to metal foil for all three concrete specimens.

The variation of equivalent mass parameter (m) is shown in Figure 16(a) to (c) for Specimens 1, 2 and 3, respectively. It can be observed that as the hydration progresses, concrete gets densified over the time due to formation cement hydrated compounds, mainly calcium sulphoaluminates, aluminohydrates, CSH gel and calcium hydroxide $\text{Ca}(\text{OH})_2$. From Figure 16, it can be observed that the PZT identified mass variation has very negligible trend in overall hydration process but slightly increases in early setting phase because concrete loses its plasticity with the progressive formation of the setting compounds ($\text{C}_6\text{A}\bar{\text{S}}_3\text{H}_{32}$, $3\text{C}_4\text{A}\bar{\text{S}}\text{H}_{12}$ and $\text{C}_4(\text{A}, \text{F})\text{H}_{13}$) (Mehta and Monteiro, 2014; Neville, 2004).

The mechanics of hydration phase can be explained for the piezo-identified mass gain as follows. When the Portland cement dispersed in water, calcium sulphate and the high-temperature compounds (C_3A and C_3S) begin to go into the solution, setting compound forms and the liquid phase rapidly gets saturated with various

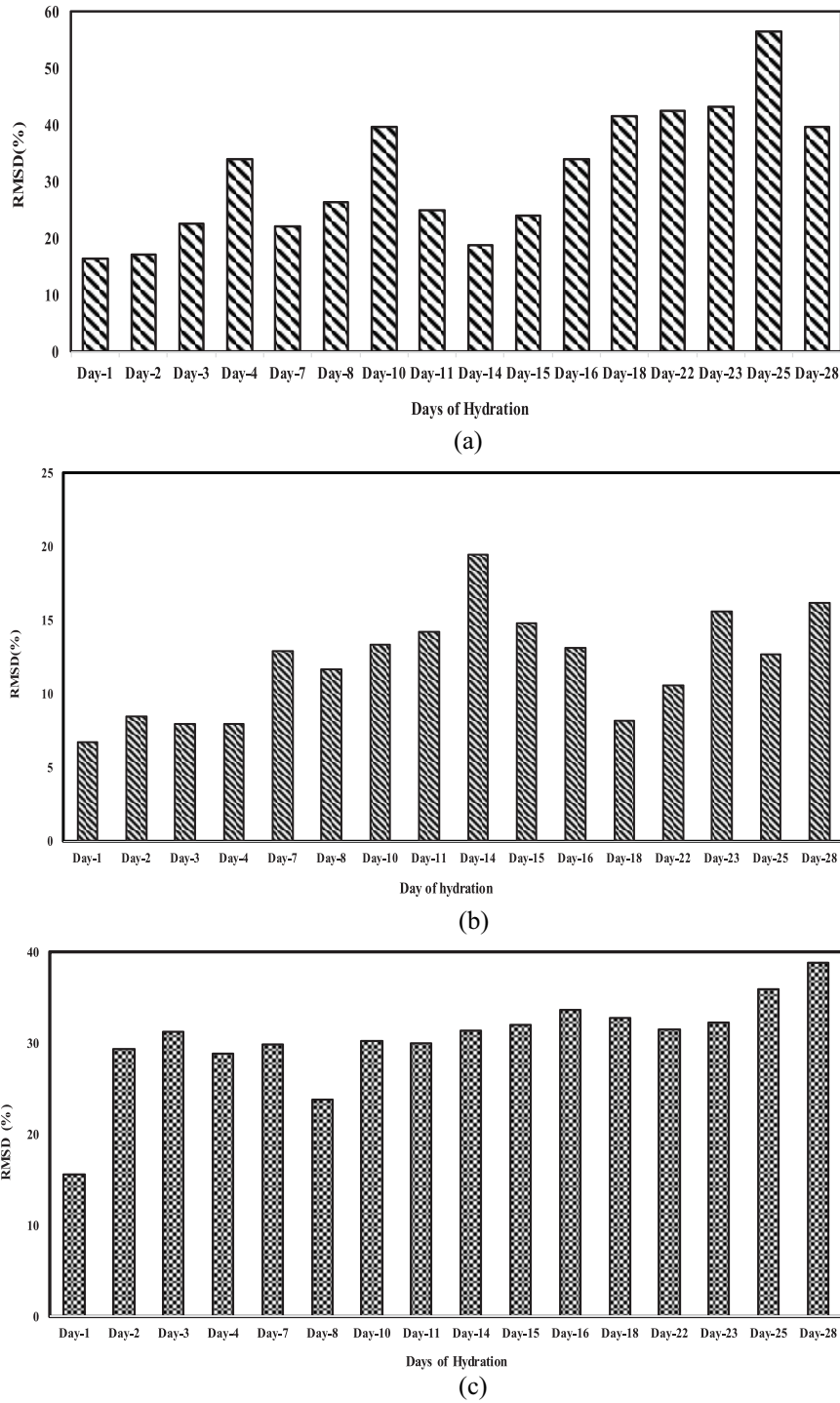


Figure 10. RMSD variation for Specimen I during hydration monitoring: (a) embedded sensor, (b) rebar bonded sensor and (c) MFBPS sensor.

ionic species. This phase lasts initial early hours. During initial hydration phase, the mass values increase slightly during early hydration hours (setting period) and later on remain constant and hardly any variation has observed. After 3 days, the ettringite decomposes to monosulphoaluminate and rapid formation CSH-short fibre makes the formation fundamental concrete

structure with stable form hydration products (Gauffinet et al., 1998; Mindess and Young, 1981). At this particular moment, concrete completely loses its plasticity, starts to fill up the water pores (reduction $\text{Ca}(\text{OH})_2$ and densification). The stated mechanism can be observed in Figure 16(a) to (c) in early hydration phase. The mass gain is very negligible from day 3

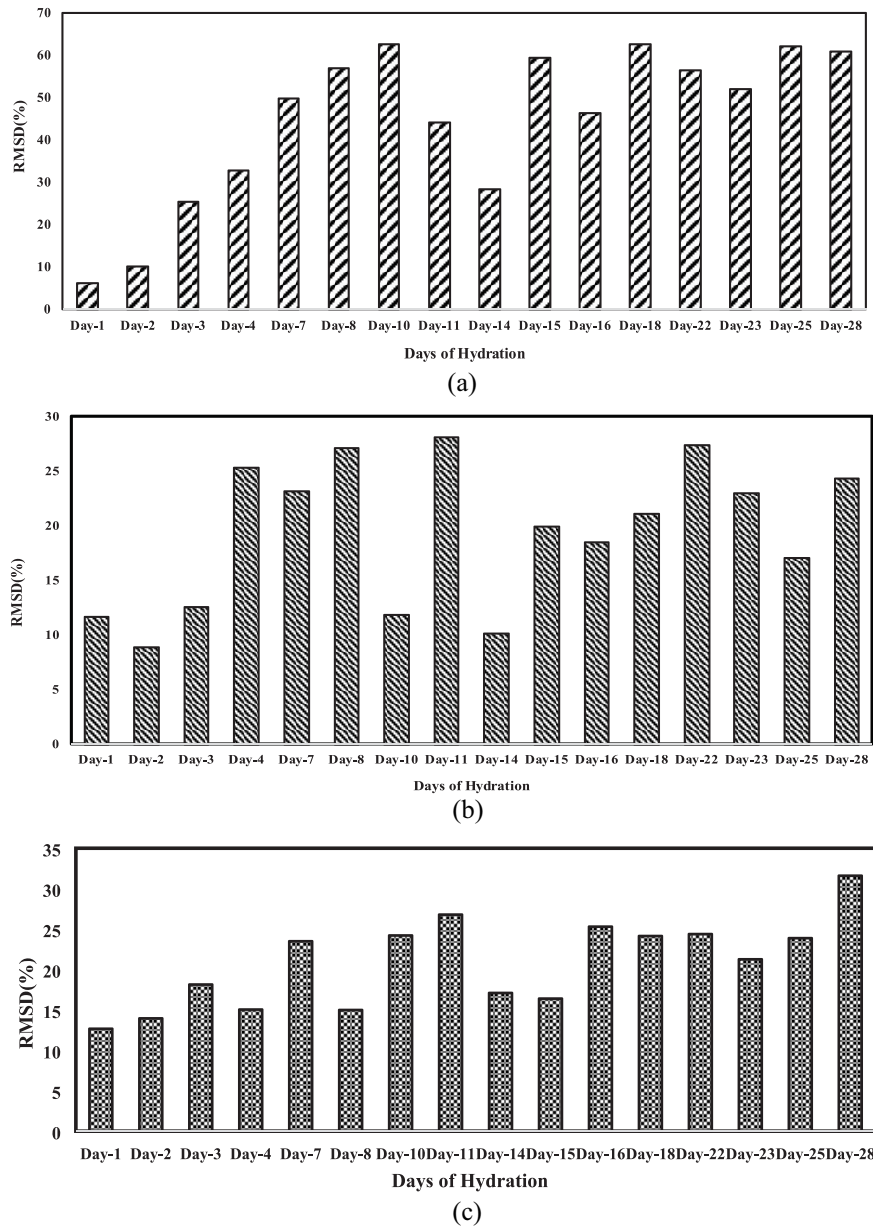


Figure 11. RMSD variation for Specimen 2 during hydration monitoring: (a) embedded sensor, (b) rebar bonded sensor and (c) MFBPS sensor.

onwards (see Figure 16(a) and (b)). As hydration progresses, large prismatic crystals of calcium hydroxide and very small fibrous crystals of CSHs begin to fill the empty space formerly occupied by water and the dissolving cement particles. At this point, concrete has attained the firm hardened shape after condensation of cement hydrated structure (Fierens and Verhaegen, 1976; Portland Cement Association (PCA), 2018), which can be seen with minute increase in mass from Figure 16 (from 20th, the day after casting till 28 days). Overall, the variation of mass is not significant for long-term hydration but in early stage, the piezo-identified mass increases during setting period of cement. The observations based on m (Figure 16) are

certainly better than those based on RMSD (Figures 10–12).

Figure 17(a) to (c) shows the variation of the equivalent stiffness (k) for Specimens 1, 2 and 3, respectively, with time. The hydration process is accompanied by the formation of strength-related compounds and bonding between them. The concerned mechanism for the stiffness can be explained as follows. During the plastic phase (first few hours), the equivalent stiffness values are significantly higher during early hydration phase (1, 3, 5, 9, 24, 48 and 72 h), which is highlighted in closer view of initial long-term hydration curve (see Figure 17(a)). This is because the concrete ingredients start ionic exchange and actively participate for setting of

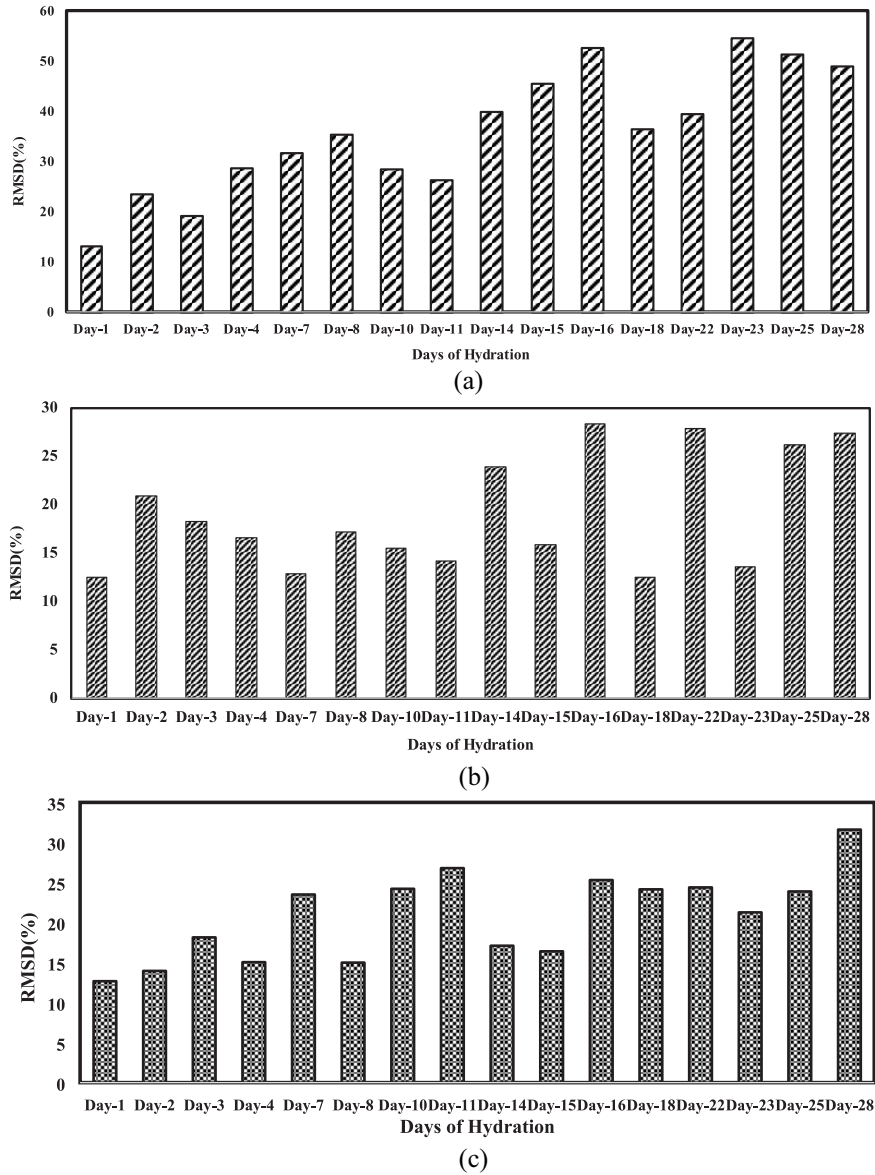


Figure 12. RMSD variation for Specimen 3 during hydration monitoring: (a) embedded sensor, (b) rebar bonded sensor and (c) MFBPS sensor.

Table 1. Mechanical impedance of combinations of spring, mass and damper.

Combination	x	y	x vs frequency	y vs frequency
	$\frac{c^{-1}}{c^{-2} + (\omega m)^{-2}}$	$\frac{m^{-1} - k(c^{-2} + \omega^{-2}m^{-2})}{\omega(c^{-2} + (\omega m)^{-2})}$		

concrete. As the reaction progresses, along with setting compound, the initial strength (long fibre-CSH) compounds start forming. Once the setting period

completes, strength compound formation continues for several weeks. The progressive filling of the void spaces in the paste with reaction products results in a decrease

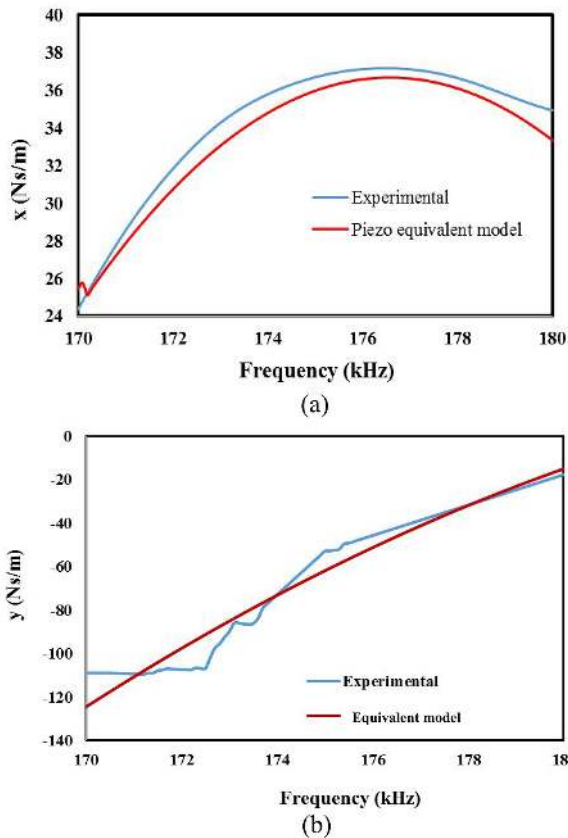


Figure 13. Validation of mechanical impedance of Specimen 1 in 170–180 kHz: (a) real part versus frequency and (b) imaginary part versus frequency.

of water filled capillary pores. With the high specific surface area (100–700 m² per gramme) and additive property of CSH (Short fibre) gel, the cement concrete converts from mineral structure to fundamental early formed structure (Kosmatka and Panarese, 1988; Mehta and Monteiro, 2014; Mindess and Young, 1981). This, indeed, is confirmed by the significant increase of the equivalent stiffness for first 3 days. This is clearly evident for Specimens 1, 2 and 3 (Figure 17(a)–(c), respectively). As the day progresses, the microstructural changes happen to attain fully strength and hardened cement concrete based on characteristic of CSH gel. Commensurate trend of piezo-identified stiffness variation (not significantly increases) around 21 days of hydration and afterwards can be observed for all the three specimens (see Figure 17(a)–(c)). Again, the variation of the equivalent stiffness is certainly much more correlative with hydration than RMSD.

Figure 18 collectively represents the variation of the piezo-identified equivalent damping parameter for Specimens 1, 2 and 3. In general, the damping behaviour of concrete is quite complicated when it transits from the plastic to the hardened state. Mostly, the damping decreases with the formation of the strength compounds and densification, which can be clearly

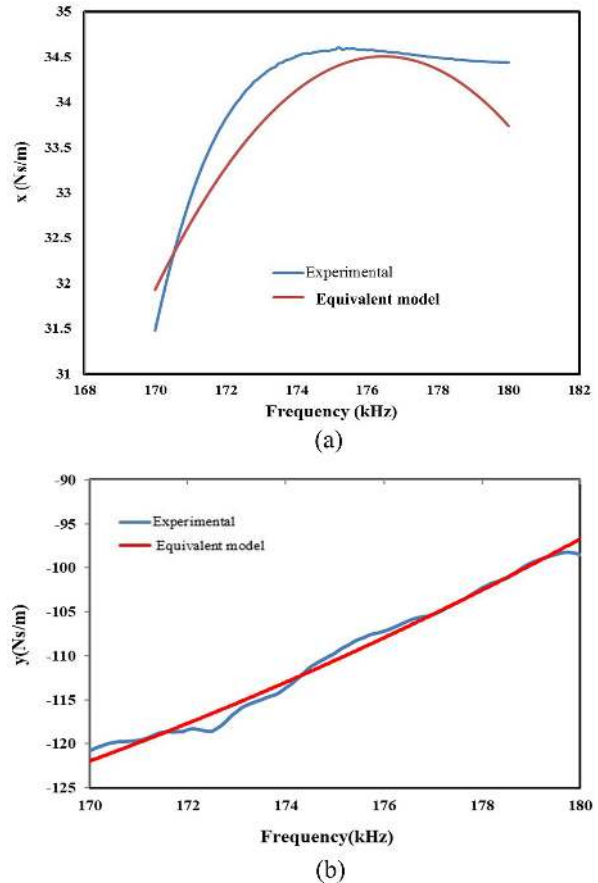


Figure 14. Validation of mechanical impedance of Specimen 2 in 170–180 kHz: (a) real part versus frequency and (b) imaginary part versus frequency.

observed in Figure 18(a) to (c) through complete hydration monitoring. In general, damping may be dependent on the small residual internal friction in the fresh concrete and can be assumed to be of a hysteretic character. Damping of homogeneous fluid is proportional to the amplitude of given dynamic force. However, for fresh concrete, in plastic state (during the initial phase of hydration), large energy absorption occurs due to the plastic deformation (Arnaud and Thinet, 2000a, 2000b). Therefore, the piezo-identified damping decreases rapidly during early hydration hours (see Figure 18(a)–(c)). After the early hydration period, the setting compounds render the concrete to loose plasticity and temperature and air tends to promote moisture loss due to evaporation. This process is also called as de-aeration stage (removal of entrapped air). During the de-aeration stage, the energy absorption decreases rapidly (Lane and Ozyildirim, 1998). Similar behaviour has been reported for piezo-identified damping values over (2–6 days), as can be clearly observed from Figure 18 for all the three concrete specimens.

After the de-aeration stage, segregation of ettringite and monosulfoaluminate introduces bonding between the paste and the aggregate (formation of CSH gel of

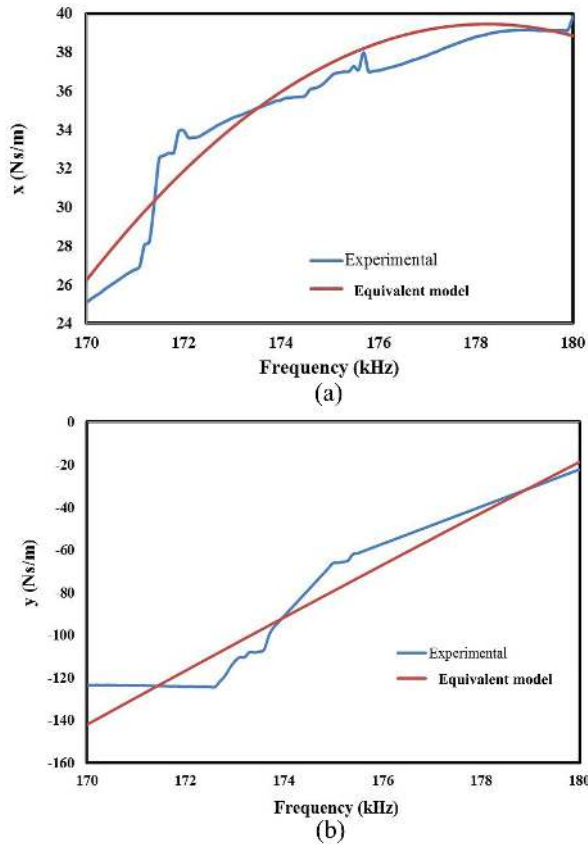


Figure 15. Validation of mechanical impedance of Specimen 3 in 170–180 kHz: (a) real part versus frequency and (b) imaginary part versus frequency.

low density). After the formation of final hardened concrete, the voids and micro cracks appear due to evaporation and shrinkage, which further more decreases the piezo-identified damping values. Hence, piezo-identified damping values decrease from 6 to 21 days of hydration as can be in Figure 18(a) to (c). The results from Sample 3 shows some abnormality but for Samples 1 and 2, piezo-identified damping values complement with cement hydration mechanism.

Again, the equivalent parameter offers far better explanation for the hydration process than the RMSD variation of other piezo configuration in specimen. From the above concrete hydration study with proposed sensor location, it is found that the new piezo location produces much agreeable result with physically observable physio-chemical changes of plain concrete and has improved sensor reading over other existing configurations (Talakokula and Bhalla, 2015; Talakokula et al., 2016).

The above analysis clearly reinforces that the piezo-identified k , m and c for the metal foil configuration are competent in realistically identifying the various stages of hydration process in concrete. Figures 19 to 21 provide a plot of parameters in non-dimensional form.

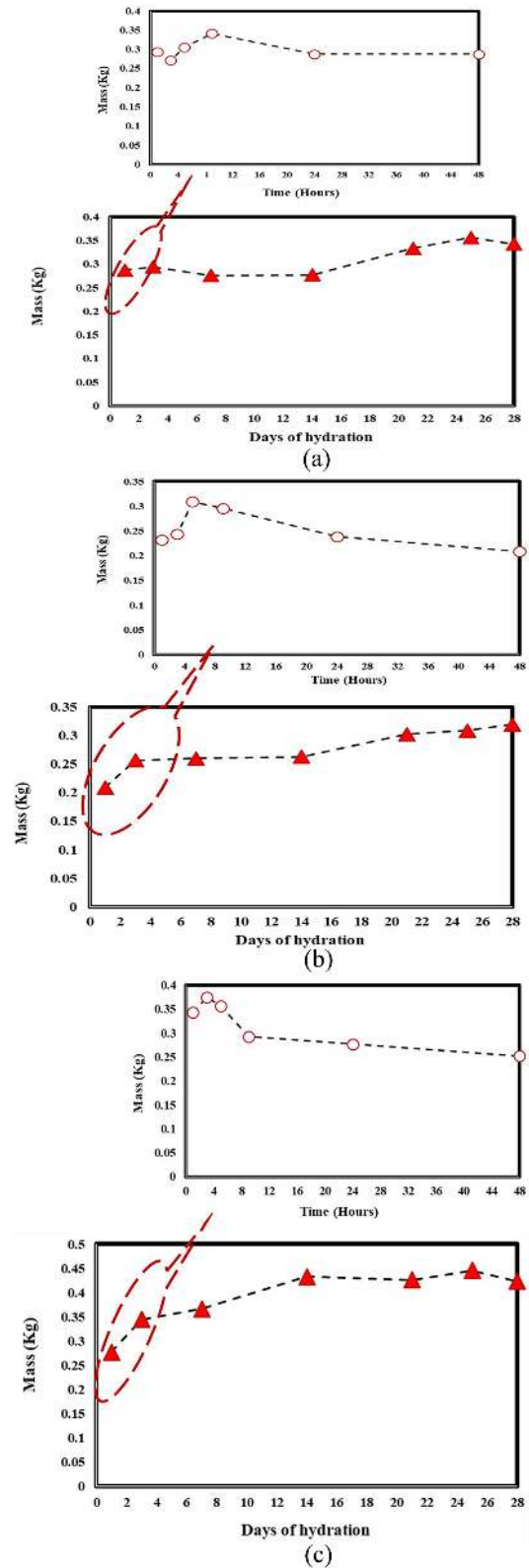


Figure 16. Variation of PZT identified equivalent mass with hydration progression: (a) Specimen 1, (b) Specimen 2 and (c) Specimen 3.

Based on these plots and the observations during the hydration-related experiments, attaining a value of 0.4

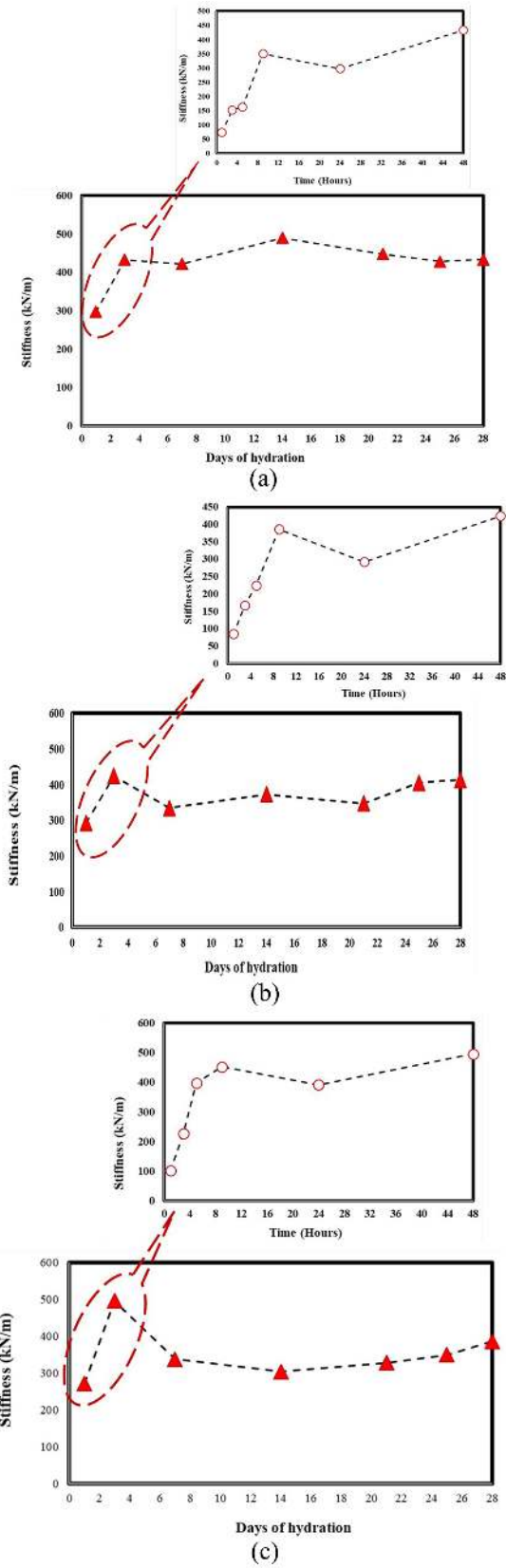


Figure 17. Variation of PZT identified equivalent stiffness with hydration progression: (a) Specimen 1, (b) Specimen 2 and (c) Specimen 3.

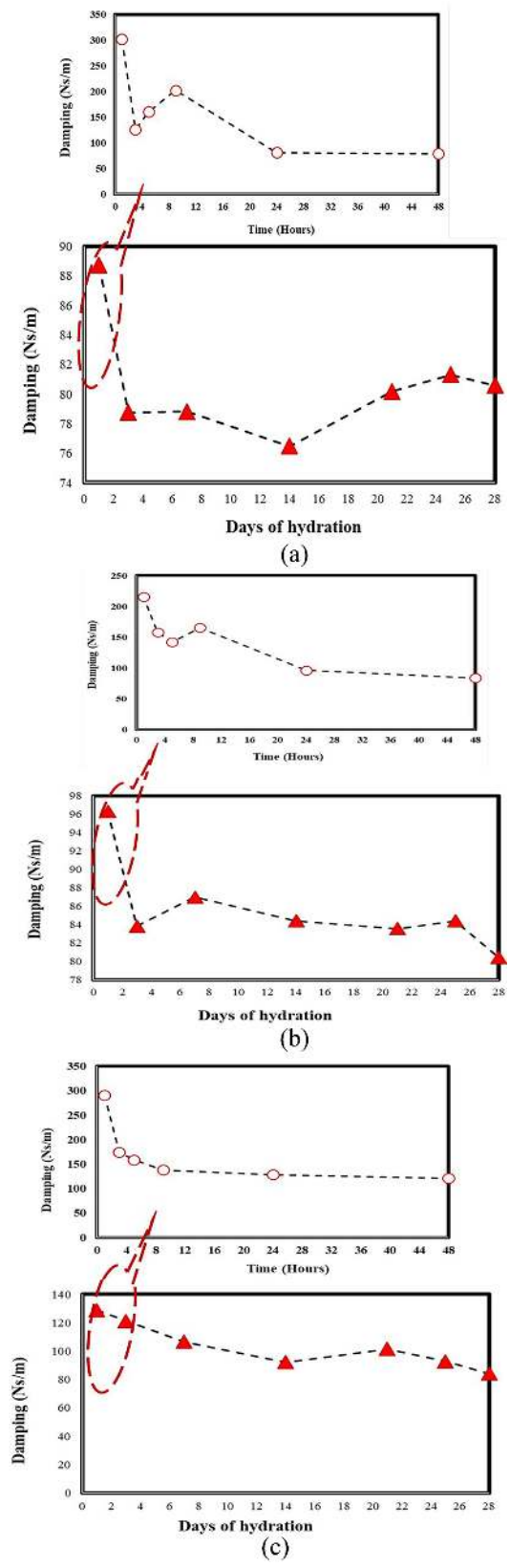


Figure 18. Variation of PZT identified equivalent damping with hydration progression: (a) Specimen 1, (b) Specimen 2 and (c) Specimen 3.

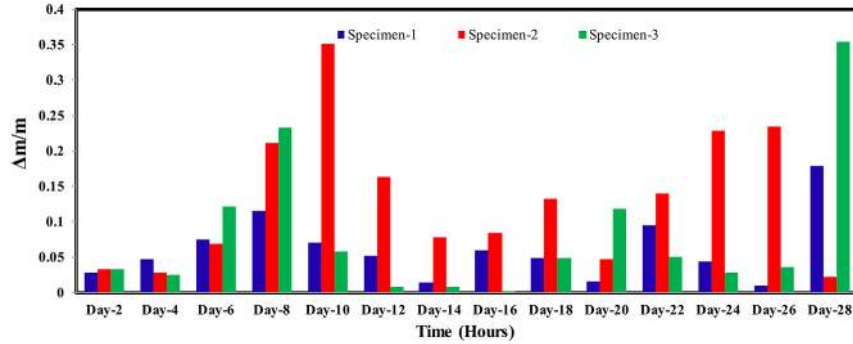


Figure 19. Variation of non-parametric ($\Delta m/m$) mass parameter with hydration.

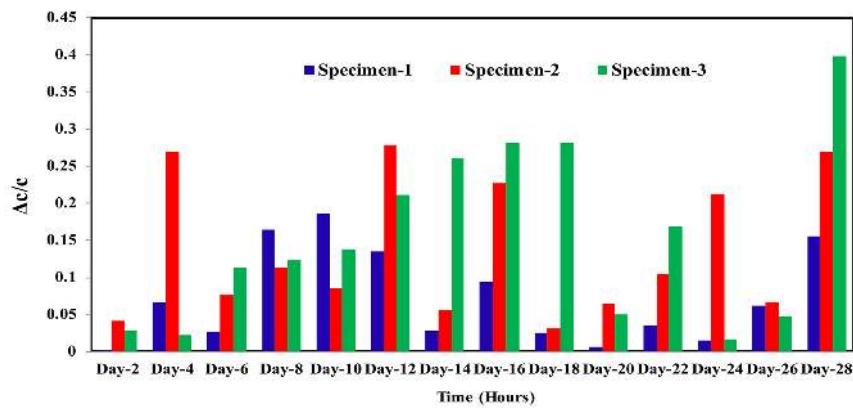


Figure 20. Variation of non-parametric ($\Delta c/c$) mass parameter with hydration.

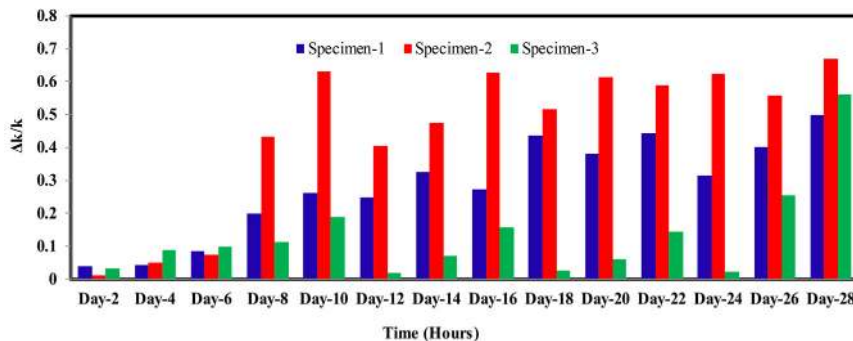


Figure 21. Variation of non-parametric ($\Delta k/k$) parameter with hydration.

by the non-dimensional parameters k , m and c provides an indication that the hydration process has reached completion level commensurate with the 28-day curing normally accepted in the concrete industry.

5. Conclusion

From the results of the present study, it is concluded that the metal foil-based configuration has significant potential and possible applicability for hydration

monitoring of concrete structures, especially where the accessibility is restricted, such as in nuclear power plants and large railway and highway bridges. The equivalent structural parameters were extracted from the piezo-coupled signature acquired by the MFBPS configuration for monitoring the physio-chemical changes in cement concrete. The study focused about exploring the ability of the metal foil-based PZT configuration to predict both the early and long-term hydration behaviour of cement-based materials and to

accurately estimate their setting time, commensurate with equivalent mass, damping and stiffness. The PZT patch attached to metal foil is able to quantitatively monitor hydration of concrete as observed from the signatures and the equivalent parameters and can be used as an appropriate technique for health monitoring of concrete structures with structural complexity. It provides a more realistic analysis as compared to the statistical RMSD index. Furthermore, based on non-dimensional mass, stiffness and damping parameters, meaningful decisions about the present stage of hydration can be easily arrived at. An appropriate time value can be observed from these results to remove the formwork from structural elements. The proposed metal foil configuration has advantages that it is reusable and at the same time much easy to implement in situ compared to other configurations, namely, the surface bonded, rebar bonded and embedded, which require skilled manpower and also rule out the possibility of reuse. It can be used for inaccessible positions of structure also. Hence, the proposed hydration-monitoring sensor has high potential in the concrete industry.


Declaration of conflicting interests

The author(s) declared no potential conflicts of interest with respect to the research, authorship and/or publication of this article.

Funding

The author(s) received no financial support for the research, authorship and/or publication of this article.

ORCID iD

Sumedha Moharana  <https://orcid.org/0000-0001-6943-5609>

References

- Arnaud R and Thinet S (2000a) A device to monitor continuously the setting of concrete (Paper ID-530). In: *15th world conference on non-destructive testing*, Rome, 15–25 October.
- Arnaud R and Thinet S (2000b) Acoustic waves to monitor the setting of hydraulic concrete: experiments and rheological analysis. *The E-Journal of Non-Destructive Testing* 6(5): 1–7.
- Azenha M, Faria R and Ferreira D (2009) Identification of early age concrete temperatures and strains monitoring and numerical simulation. *Cement and Concrete Composite* 31(6): 369–378.
- Bahador SD and Yaowen Y (2010) Monitoring hydration of concrete with piezoelectric transducer. In: *35th conference on our world in concrete & structures*, Singapore, 25–27 August.
- Banerjee S, Ricci F, Monaco E, et al. (2009) A wave propagation and vibration-based approach for damage identification in structural components. *Journal of Sound and Vibration* 332(1–2): 167–183.
- Bhalla S and Gupta A (2007) Novel Vibration Sensor for Concrete Structures (Patent application no. 1011/DEL/2011, Invention disclosure (FT/IPR/CE/SB/2007/0570)). New Delhi, India: Foundation for Innovation and Technology Transfer (FITT), IIT Delhi.
- Bhalla S and Soh CK (2004a) Impedance based modelling for adhesively bonded piezo-transducers. *Journal of Intelligent Material Systems and Structure* 15(12): 955–972.
- Bhalla S and Soh CK (2004b) Structural health monitoring by piezo-impedance transducers I: modelling. *Journal of Aerospace Engineering* 17(4): 154–165.
- Bhalla S and Soh CK (2004c) Structural health monitoring by piezo-impedance transducers II: application. *Journal of Aerospace Engineering* 17(4): 166–175.
- Bhalla S, Moharana S, Talakokula V, et al. (2017) *Piezoelectric Materials: Applications in SHM, Energy Harvesting and Biomechanics*. New Delhi: Wiley and Athena Academics.
- Bhalla S, Vittal APR and Veljkovic M (2012) Piezo-impedance transducers for residual fatigue life assessment of bolted steel joints. *Structural Health Monitoring: An International Journal* 11(6): 733–750.
- Cheol KW and Park G (2016) Experimental and numerical validation of the technique for concrete cure monitoring using piezoelectric admittance measurements. *Journal of the Korean Society for Nondestructive Testing* 36: 217–224.
- Constantin EC, Chris GK, Angelia GM, et al. (2016) Applications of smart piezoelectric materials in a wireless admittance monitoring system (WIAMS) to structures – tests in RC element. *Case Studies in Construction Materials* 5: 1–18.
- Fierens P and Verhaegen JP (1976) Hydration of tricalcium silicate in paste-kinetics of calcium ion dissolution in the aqueous phase. *Cement and Concrete Research* 6: 337–342.
- Gauffinet S, Finot Lesniewska ÉE and Nonat A (1998) Observation directe de la croissance d'hydrosilicate de calcium sur des surfaces d'alite et de silice par microscopie a force atomique. *Comptes Rendus de l'Academie de Sciences. Serie IIa: Sciences de la Terre et des Planetes* 327: 231–236.
- Giurgiutiu V and Zagrai AN (2000) Characterization of piezoelectric wafer active sensors. *Journal of Intelligent Material Systems and Structures* 11: 959–976.
- Giurgiutiu V and Zagrai AN (2002) Embedded self-sensing piezoelectric active sensors for on-line structural identification. *Journal of Vibration and Acoustics* 124: 116–125.
- Glisic B and Inaudi D (2006) Monitoring of early and very early age deformation of concrete using concrete using fiber optics sensors (Paper ID 17–26 (#614)). In: *Proceedings of the 2nd international congress*, Naples, 5–8 June.
- Glisic B and Simon N (1999) Monitoring of concrete at very early age using SOFO sensor. *Cement and Concrete Composite* 22(2): 115–119.
- Hixon EL (1988) Mechanical impedance. In: Harris CM (Ed.) *Shock and Vibration Handbook*. 3rd ed. New York: McGraw-Hill, pp. 10.1–10.46.
- IS 10262 (2009) *Concrete Mix Proportioning – Guidelines*. New Delhi, India: Bureau of Indian Standards.
- IS 383 (1970) *Specification for Coarse and Fine Aggregates from Natural Sources for Concrete*. New Delhi, India: Bureau of Indian Standards.

- Jung KH, Jo HJ, Park G, et al. (2014) Relative baseline features for impedance-based structural health monitoring. *Journal of Intelligent Material Systems and Structures* 25: 2294–2304.
- Kaur N and Bhalla S (2015) Combined energy harvesting and structural health monitoring potential of embedded piezo-concrete vibration sensors. *Journal of Energy Engineering* 141(4): D4014001-18.
- Kim WC, Jo HJ and Park G (2015) Concrete cure monitoring using piezoelectric admittance measurements. In: *Proceedings of the 2015 world congress on advances in structural engineering and mechanics*, Incheon, Korea, 25–29 August.
- Kong D, Hou S, Qing J, et al. (2013) Very early age concrete hydration characterization monitoring using piezoceramic based smart aggregates. *Smart Materials and Structures* 22(8): 085025.
- Kosmatka S and Panarese W (1988) *Design and Control of Concrete Mixes*. Skokie, IL: Portland Cement Association.
- Lane RO and Ozyildirim PH (1998) Behaviour of fresh concrete under vibration. *ACI Committee Report*. Available at: http://civilwares.free.fr/ACI/MCP04/3091r_93.pdf
- Lee HK and Tawie R (2009) Monitoring strength gain of concrete using EMI sensing technique. In: *Proceeding of the sensors and smart structures technologies for civil, mechanical, and aerospace systems* (eds Y Chung-Bang, V Giurgiutiu and M Tomizuka), vol. 7292, p. 729223. Bellingham, WA: SPIE.
- Lim YY (2014) Monitoring of concrete hydration using electromechanical impedance technique. In: *Australasian conference on the mechanics of structures and materials (ACMSM23)*, vol. 23, Byron Bay, NSW, Australia, 9–12 December.
- Lim YY, Bhalla S and Soh CK (2006) Structural identification and damage diagnosis using self-sensing piezo-impedance transducers. *Smart Materials and Structures* 15(4): 987–995.
- Lim YY, Kwong ZK, Liew WYH, et al. (2016) Non-destructive concrete strength evaluation using smart piezoelectric transducer – a comparative study. *Smart Materials and Structures* 25: 085021.
- Lim YY, Kwong ZK, Liew WYH, et al. (2018a) Parametric study and modelling of PZT based wave propagation technique related to practical issues in monitoring of concrete curing. *Construction and Building Materials* 176: 519–6530.
- Lim YY, Smith S and Soh CK (2018b) Wave propagation based monitoring of concrete curing using piezoelectric materials: review and path forward. *NDT & E International* 99: 50–63.
- Lu X, Lim YY and Soh CK (2017) A novel electromechanical impedance-based model for strength development monitoring of cementitious materials. *Structural Health Monitoring: An International Journal* 17: 902–918.
- Lu X, Lim YY and Soh CK (2018) Investigating the performance of ‘smart probe’ based indirect EMI technique for strength development monitoring of cementitious materials – modelling and parametric study. *Construction and Building Materials* 172: 134–152.
- Mascarenas DDL, Eric FB, Todd M, et al. (2010) Development of capacitance-based and impedance-based wireless sensors and sensor nodes for structural health monitoring applications. *Journal of Sound and Vibration* 329: 2410–2420.
- Mehta PK and Monteiro PJM (2014) *Concrete: Microstructure, Properties, and Materials*. 4th ed. New York: McGraw-Hill.
- Mindess S and Young JF (1981) *Concrete*. Englewood Cliffs, NJ: Prentice Hall.
- Moharana S and Bhalla S (2014) A continuum based modelling approach for adhesively bonded piezo-transducers for EMI technique. *International Journal of Solids and Structures* 51(6): 1299–1310.
- Moharana S and Bhalla S (2015) Influence of adhesive bond layer on power and energy efficiency of piezo-impedance transducer. *Journal of Intelligent Material Systems and Structures* 26(3): 247–259.
- Na S and Lee HK (2013) Steel wire electromechanical impedance method using a piezoelectric material for composite structures with complex surfaces. *Composite Structures* 98: 79–84.
- Naskar S and Bhalla S (2015) Metal wire based twin 1D orthogonal array configuration of PZT patches for damage assessment of 2D structures. *Journal of Intelligent Material Systems and Structures* 27(11): 1440–1460.
- Neville AM (2004) *Properties of Concrete*. 4th ed. Philadelphia, PA: Trans-Atlantic Publications.
- Ni X, Rizzo P, Yang J, et al. (2012) Monitoring the hydration of cement using highly nonlinear solitary waves. *NDT & E International* 52: 76–85.
- Park G, Cudney HH and Inman DJ (2000a) An integrated health monitoring technique using structural impedance sensors. *Journal of Intelligent Material Systems and Structures* 11: 448–455.
- Park G, Cudney HH and Inman DJ (2000b) Impedance-based health monitoring of civil structural components. *Journal of Infrastructure System* 6(4): 153–160.
- Park G, Inman DJ and Farrar CR (2003) Recent studies in piezoelectric impedance-based structural health monitoring. In: *Proceedings of 4th international workshop on structural health monitoring: From diagnostics and prognostics to structural health management*, Stanford University, Palo Alto, CA, 15–17 September, pp. 1423–1430. Lancaster, PA: DES Tech Publications.
- Park S, Lee JJ, Yun CB, et al. (2008) Electro-mechanical impedance-based wireless structural health monitoring using PCA-data compression and K-means clustering algorithms. *Journal of Intelligent Material Systems and Structures* 19: 509–520.
- PI Ceramics (2017) *Product Information Catalogue*. Lederhose: PI Ceramics. Available at: <https://www.piceramic.com/en/products/piezoceramic-materials/> (accessed 15 July 2017).
- Portland Cement Association (PCA) (2017). Education. Available at: <https://www.cement.org/learn/education>
- Providakis CV and Liarakos EV (2014) Web-based concrete strengthening monitoring using an innovative electromechanical impedance telemetric system and extreme values statistics. *Structural Control and Health Monitoring* 21(9): 1252–1268.
- Shanker R, Bhalla S and Gupta A (2011) A dual use of PZT patches as sensors in global dynamic and local EMI techniques for structural health monitoring. *Journal of Intelligent Material Systems and Structures* 22(16): 1841–1856.
- Shin SW and Oh TK (2009) Application of electro-mechanical impedance sensing technique for online monitoring of

- strength development in concrete using smart PZT patches. *Construction and Building Materials* 23(2): 1185–1188.
- Shin SW, Qureshi AR, Lee JY, et al. (2008) Piezoelectric sensor based non-destructive active monitoring of strength gain in concrete. *Smart Materials and Structures* 17: 055002.
- Sikdar S and Banerjee S (2016) Ultrasonic guided wave propagation and disbond identification in a honeycomb composite sandwich structure using bonded piezoelectric wafer transducers. *Journal of Intelligent Materials Systems and Structures* 27(13): 1767–1779.
- Soh CK and Bhalla S (2005) Calibration of piezo-impedance transducers for strength prediction and damage assessment of concrete. *Smart Materials and Structures* 14(4): 671–684.
- Soh CK, Tseng KKH, Bhalla S, et al. (2000) Performance of smart piezoceramic patches in health monitoring of a RC bridge. *Smart Materials and Structures* 9(4): 533–542.
- Su H, Zhang N, Wen Z, et al. (2016) Experimental study on obtaining hydraulic concrete strength by use of concrete piezoelectric ceramic smart module pairs. *Journal of Intelligent Material Systems and Structures* 27(5): 666–678.
- Sun FP, Chaudry Z, Rogers CA, et al. (1995) Automated real-time structure health monitoring via signature pattern recognition. In: *Smart structures and materials 1995: Smart structures and integrated systems*, San Diego, CA, 27 February–1 March, pp. 236–247. Bellingham, WA: SPIE.
- Talakokula V and Bhalla S (2015) Reinforcement corrosion assessment capability of surface bonded and embedded piezo sensors for RC structures. *Journal of Intelligent Material System and Structures* 26(17): 2304–2313.
- Talakokula V, Bhalla S and Gupta A (2014) Corrosion assessment of RC structures based on equivalent structural parameters using EMI technique. *Journal of Intelligent Material Systems and Structures* 25(4): 484–500.
- Talakokula V, Bhalla S and Gupta A (2018) Monitoring early hydration of reinforced concrete structures using structural parameters identified by piezo sensors via electromechanical impedance technique. *Mechanical Systems and Signal Processing* 99: 129–141.
- Talakokula V, Bhalla S, Ball RJ, et al. (2016) Diagnosis of carbonation induced corrosion initiation and progression in reinforced concrete structures using piezo-impedance transducers. *Sensors and Actuators A: Physical* 242: 79–91.
- Tawie R and Lee HK (2010) Piezoelectric-based non-destructive monitoring of hydration of reinforced concrete as an indicator of bond development at the steel-concrete interface. *Cement and Concrete Research* 40(12): 1697–1703.
- Tawie R and Lee HK (2011) Characterization of cement-based materials using a reusable piezoelectric impedance-based sensor. *Smart Materials and Structures* 20: 085023.
- Tawie R, Lee HK and Park S (2010a) Non-destructive evaluation of concrete quality using PZT transducers. *Smart Structures and Systems* 6(7): 851–857.
- Tawie R, Lee HK, Min J, et al. (2010b) Monitoring hydration characteristics of cement paste by EMI method. In: Oh BH, Choi OC, Chung L, et al. (eds) *Fracture Mechanics of Concrete and Concrete Structures – Assessment, Durability, Monitoring and Retrofitting of Concrete Structures*. Seoul, South Korea: Korea Concrete Institute, pp. 1179–1180.
- Tawie R, Na S and Lee HK (2013) A study of reusable electromechanical impedance methods for structural health monitoring of civil structures. In: Lynch JP, Yun C-B and Wang K-W (eds) *Sensors and Smart Structures Technologies for Civil, Mechanical, and Aerospace Systems*, vol. 8692. Bellingham, WA: SPIE, p. 869235.
- Thiyagarajan JS, Balamonica K, Priya B, et al. (2017) Piezoelectric EMI-based monitoring of early strength gain in concrete and damage detection in structural components. *Journal of Infrastructure Systems* 23: 04017029.
- Wang DS and Zhu HP (2011) Monitoring of the strength gain of concrete using embedded PZT impedance transducer. *Construction and Building Materials* 25(9): 3703–3708.
- Yang Y, Lim YY and Soh CK (2008) Practical issues related to the application of the electromechanical impedance technique in the structural health monitoring of civil structures: I. Experiment. *Smart Materials and Structures* 17: 035008.
- Yang Y, Lim YY, Annamdas VG, et al. (2012) Sensing region, load monitoring and practical issues. In: Soh CK, Yang Y and Bhalla S (eds) *Smart Materials in Structural Health Monitoring, Control and Biomechanics*. Berlin; Heidelberg: Springer, pp. 245–297.